The Inositol 1,4,5-Trisphosphate Receptor of Cerebellum

Mn^{2+} Permeability and Regulation by Cytosolic Mn^{2+}

FRANK STRIGGOW and BARBARA E. EHRLICH

From the Departments of Physiology and Medicine, University of Connecticut Health Center, Farmington, Connecticut 06030-3505

ABSTRACT The inositol 1,4,5-trisphosphate receptor ($InsP_3R$), an intracellular calcium release channel, is found in virtually all cells and is abundant in the cerebellum. We used Mn^{2+} as a tool to study two aspects of the cerebellar $InsP_3R$. First, to investigate the structure of the ion pore, Mn^{2+} permeation through the channel was determined. We found that Mn^{2+} can pass through the $InsP_3R$; the selectivity sequence for divalent cations is $Ba^{2+} > Sr^{2+} > Ca^{2+} > Mg^{2+} > Mn^{2+}$. Second, to begin characterization of the cytosolic regulatory sites responsible for the Ca^{2+}-dependent modulation of $InsP_3R$ function, the ability of Mn^{2+} to replace Ca^{2+} was investigated. We show that Mn^{2+}, as Ca^{2+}, modulates $InsP_3R$ activity with a bell-shaped dependence where the affinity of the activation site of the $InsP_3R$ is similar for both ions, but higher concentrations of Mn^{2+} were necessary to inhibit the channel. These results suggest that the two regulatory sites are structurally distinct. Our findings are also important for the understanding of cellular responses when Mn^{2+} is used to quench the intracellular fluorescence of Ca^{2+} indicator dyes. Key words: ion permeation • ion selectivity • calcium release channel • fura-2

INTRODUCTION

A Ca^{2+} flux through the inositol 1,4,5-trisphosphate receptor ($InsP_3R$)[1] from the lumen of the endoplasmic reticulum to the cytosol constitutes an important step in intracellular Ca^{2+} signaling. This signaling cascade is stimulated by the binding of an agonist to its receptor on the outer surface of the plasma membrane followed by the activation of a phospholipase C and the formation of diacylglycerol and inositol 1,4,5-trisphosphate ($InsP_3$) (Berridge, 1993; Clapham, 1995). The density of the $InsP_3R$ is highest in the cerebellum, specifically in the Purkinje cells (Supattapone et al., 1988), and the majority of biochemical, molecular, and biophysical studies of this channel have used the cerebellar receptor. Models have been proposed and experimental evidence is accumulating suggesting that the $InsP_3R$ is involved in intercellular signaling between neuronal cells (Charles, 1994; Sneyd et al., 1995) and long term potentiation (Malenka, 1994).

It has been shown recently that the $InsP_3R$ selects weakly among the alkaline earth cations (Bezprozvanny and Ehrlich, 1994). The permeation sequence decreases in the order $Ba^{2+} > Sr^{2+} > Ca^{2+} > Mg^{2+}$. The first issue addressed here is whether Mn^{2+} as a transition metal is also able to pass through the $InsP_3R$. The answer to this question would allow conclusions concerning the mechanism of ion translocation though the channel pore of the $InsP_3R$.

The steady state activity of the $InsP_3$-gated channel follows the cytosolic Ca^{2+} concentration with a bell-shaped dependence, where maximal activation occurs at ~200 nM free Ca^{2+} (Iino, 1990; Bezprozvanny et al., 1991; Finch et al., 1991). At least two cytosolic Ca^{2+} binding sites are responsible for the Ca^{2+}-induced activation and inhibition of the $InsP_3R$ (Bezprozvanny et al., 1991; Marshall and Taylor, 1994). The second issue of this study is to characterize these binding sites by investigating the ability of Mn^{2+} to replace Ca^{2+} in modulating the channel activity.

In addition to conclusions concerning properties of the channel pore and the Ca^{2+}-dependent regulatory sites of the $InsP_3R$, both questions posed in the present paper may be important for studies of intracellular Ca^{2+} homeostasis in neurons and other cells. Because of its ability to quench the fluorescence of different Ca^{2+} indicator dyes (e.g., fura-2, indo-1), Mn^{2+} has become a useful tool for investigating intracellular Ca^{2+} signaling, especially for discriminating between the activation of a Ca^{2+} influx channel in the plasma membrane (which is also permeable for Mn^{2+}) and the release of Ca^{2+} from intracellular stores (Merritt et al., 1989). More recently, Mn^{2+} has also been used to study or to detect the $InsP_3R$ by quenching intraorganellar (endoplasmic reticulum, nuclear cisterna) dye fluorescence (Hajnoczky and Thomas, 1994; Stehno-Bittel et al., 1995*b*). The latter type of experiment assumes that Mn^{2+} is able to permeate through the $InsP_3R$ when the channel is activated by $InsP_3$. However, Mn^{2+} permeation through the $InsP_3R$ had not been shown directly. Furthermore, the ability of Mn^{2+} itself to alter the activ-

Address correspondence to Dr. Frank Striggow, Department of Physiology, University of Connecticut Health Center, 263 Farmington Avenue, Farmington, CT 06030-3505. Fax: 860-679-3346; E-mail: fstriggo@neuron.uchc.edu

[1] *Abbreviations used in this paper*: $InsP_3$, inositol 1,4,5-trisphosphate; $InsP_3R$, $InsP_3$ receptor.

J. GEN. PHYSIOL. © The Rockefeller University Press • 0022-1295/96/08/115/10 $2.00
Volume 108 August 1996 115–124

ity of the $InsP_3$-gated channel by interacting with the cytosolic Ca^{2+} binding sites would have implications for both kinds of quenching experiments.

To study the Mn^{2+} permeation through the $InsP_3R$ as well as the effect(s) of Mn^{2+} on the cytosolic regulatory domains of the $InsP_3R$, we incorporated the native $InsP_3R$ from canine cerebellum into planar lipid bilayers and measured single-channel currents under voltage clamp conditions. We found that (*a*) the $InsP_3R$ is permeable to Mn^{2+}, although the conductance for this ion is lower than that observed for other divalent cations, and (*b*) cytosolic Mn^{2+} regulates the activity of the $InsP_3R$ in a bell-shaped manner.

METHODS

Preparation of Microsomes from Canine Cerebellum

Cerebella were taken from anesthetized dogs, immediately frozen in liquid nitrogen and stored at −72°C until microsomes were prepared as described previously (Watras et al., 1991). Briefly, a cerebellum was minced with scissors and then homogenized using a glass Teflon® homogenizer in 60 ml of ice-cold buffer A containing 20 mM HEPES, pH 7.35, 100 μM EDTA, and 1 μg/ml each of leupeptin and pepstatin A (both from Sigma Chemical Co., St. Louis, MO). After the addition of another 60 ml of buffer A, the suspension was centrifuged for 20 min at 4.3k *g* (45 Ti rotor; Beckman Instruments, Inc., Fullerton, CA). The supernatant was filtered through four layers of cheese cloth and the filtrate was centrifuged for 30 min at 90k *g*. The pellet from the latter spin was resuspended in 50 ml of buffer A. The resuspension was centrifuged for 20 min at 4.3k *g*. The resulting supernatant was centrifuged for 30 min at 90k *g*. The final pellet was then resuspended in 2 ml of 10% sucrose, 20 mM MOPS, pH 6.8, and 1 μg/ml each of leupeptin and pepstatin A, frozen in small aliquots in liquid nitrogen and stored at −72 °C until use. Experiments were performed with two different cerebellar microsomal preparations.

Reconstitution of the $InsP_3R$ into Planar Lipid Bilayers

Microsomes were fused with planar lipid bilayers made from 40 mg/ml phosphatidylethanolamine and phosphatidylserine (3:1; Avanti Polar Lipids Inc., Alabaster, AL) dissolved in decane. Bilayers were formed by painting the lipid solution across a 200-μm hole in a Teflon® sheet that bisected a lucite chamber. The hole was prepainted with a solution of phosphatidylcholine and phosphatidylserine (3:1) in decane (20 mg/ml) before the formation of the bilayer. Vesicles (2 μl) were added to the *cis* chamber, which contained 250 mM HEPES/Tris, pH 7.35. The *trans* chamber contained 55 mM $Ba(OH)_2$ or 55 mM $MnSO_4$ dissolved in 250 mM HEPES/Tris, pH 7.35, and was held at virtual ground. KCl was added to the *cis* chamber in steps of 0.3 M to establish an osmotic gradient between *cis* and *trans* chambers with the aim to induce fusion of the microsomes with the bilayer. Solutions in both chambers were stirred until current deflections due to the activity of K^+ and/or Cl^- channels were observed. These deflections indicated fusion of microsomes with the bilayer. After several fusion events, the *cis* chamber was perfused with 10 vol of HEPES/Tris, pH 7.35, leaving only Ba^{2+} or Mn^{2+} as a charge carrier in the *trans* chamber. The vesicles inserted into the bilayer such that the *cis* and *trans* chambers corresponded to the cytosol and to the lumen of the endoplasmic reticulum, respectively. To activate the $InsP_3R$, 0.5 mM ATP and 2 μM $InsP_3$ were added to the *cis* chamber (Bezprozvanny and Ehrlich, 1993). All subsequent compounds were added to the *cis* chamber, and the solutions in both chambers were stirred for at least 30 s after each addition. $InsP_3$-gated channel openings were observed in ~33% of the experiments. Currents were recorded using a patch clamp amplifier (PC-503; Warner Instruments Corp., Hamden, CT) under voltage clamp conditions. All experiments were performed at room temperature (20°C).

To adjust the free concentration of Ca^{2+} or Mn^{2+} on the cytosolic side of the $InsP_3R$, solutions of $CaCl_2$ (20 mM) or $MnSO_4$ (2 or 20 mM) were added to a solution containing 1 mM EGTA and 0.5 mM ATP. The final concentration of free ions was calculated using the following apparent association constants for the ion–chelator complexes given in parentheses: $1.229 \times 10^7\ M^{-1}$ (Ca^{2+}-EGTA), $2.266 \times 10^8\ M^{-1}$ (Mn^{2+}-EGTA), $6.405 \times 10^3\ M^{-1}$ (Ca^{2+}-ATP), and $2.168 \times 10^4\ M^{-1}$ (Mn^{2+}-ATP) at pH 7.35 and at 20°C (Fabiato, 1988). The total Ca^{2+} concentration of the solutions used was determined by atomic absorption spectroscopy (Galbraith Laboratories Inc., Knoxville, TN).

Analysis

Experiments were stored on video tapes and analyzed using pClamp 6.02 (Axon Instruments, Inc., Foster City, CA). For computer analysis, data were filtered to 1 kHz with an eight-pole Bessel filter and digitized at 5 kHz. Acquired data were filtered using a digital Gaussian filter with a cut-off frequency of 500 Hz. Only events longer than 2 or 3 ms were used for the calculation of open time and current amplitude, respectively. The number of $InsP_3$-gated channels in the bilayer was estimated as the maximal number of simultaneously open channels in the experiment (Horn, 1991). To compare different experiments, we normalized the open probability to the maximum open probability observed in each experiment. In all cases data are presented as mean ± SEM.

RESULTS

Mn^{2+} Permeability of the $InsP_3R$

The ability of Mn^{2+} to permeate through the $InsP_3R$ was tested to extend our knowledge of the ion selectivity sequence of this channel. To make these measurements, cerebellar microsomes were fused with planar lipid bilayers, and the currents generated with Ba^{2+} or Mn^{2+} as the current carrier were compared. The Ba^{2+} or Mn^{2+} concentration was set to 55 mM on the luminal (*trans*) side of the bilayer. With either ion, single-channel currents were activated by the addition of 0.5 mM ATP, 160 nM Ca^{2+}, and 2 μM $InsP_3$ to the cytosolic (*cis*) side of the bilayer (Fig. 1). In all experiments, $InsP_3$ was absolutely necessary for channel activation. Currents were not observed after the addition of ATP and/or Ca^{2+} in the absence of $InsP_3$ (Fig. 1, *A* and *B*, *top two traces*). Current deflections were observed only after subsequent addition of $InsP_3$ (Fig. 1, *A* and *B*, *third traces*). Heparin (10 μg/ml), a competitive inhibitor of the $InsP_3R$ (Ghosh et al., 1988), caused an immediate and complete block of channel activity (Fig. 1, *A* and *B*, *bottom traces*). When Mn^{2+} was the charge carrier, the current amplitude was significantly smaller than that measured with Ba^{2+} as the charge carrier (Fig. 2, compare panels *A* and *C*; Table I). The activation by $InsP_3$

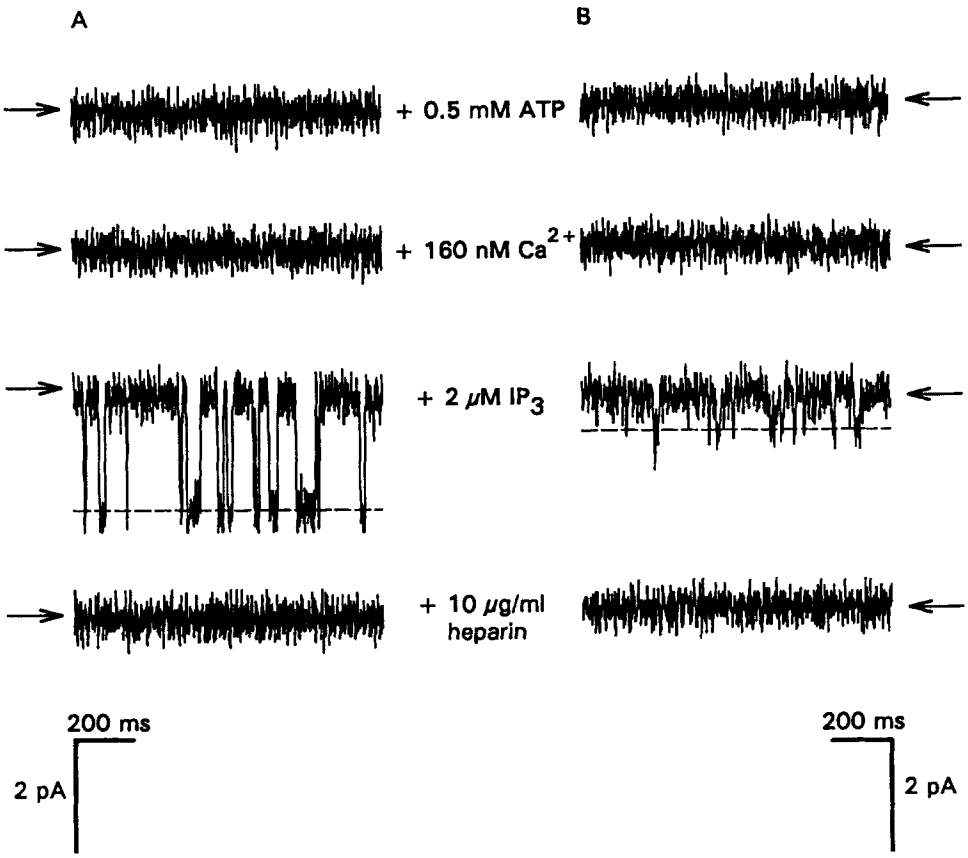

FIGURE 1. $InsP_3R$ from cerebellum in planar lipid bilayers. Currents were monitored in the presence of (*A*) 55 mM Ba^{2+} or (*B*) 55 mM Mn^{2+} on the luminal side of the $InsP_3R$. In the absence of $InsP_3$ currents were not observed after the addition of ATP (*top trace*) and/or Ca^{2+} (*second trace*). The addition of $InsP_3$ (*third trace*) was absolutely necessary to induce channel activity. Recordings were done under voltage clamp conditions at a transmembrane potential of 0 mV; channel openings are indicated as downward deflections. Arrows represent the zero current line, and the open channel current amplitude is shown by dashed lines (see Table I for the average value from four experiments). Channel activity was immediately and completely inhibited by heparin (*bottom trace*), indicating that the observed currents were generated by openings of the $InsP_3R$.

as well as the complete inhibition by heparin indicated that the observed small currents were caused by Mn^{2+} going through the $InsP_3R$. At all voltages tested, the currents were larger with Ba^{2+} as the current carrier (Fig. 3). The slope conductance for the single-channel openings measured between 0 and −40 mV was 17 pS for Mn^{2+} and 88 pS for Ba^{2+} (Fig. 3).

Further comparisons showed that the mean open time of the $InsP_3R$ was significantly shorter when Mn^{2+} was the permeating ion (Fig. 2, compare panels *B* and *D*; Table I). The mean open time for Ba^{2+} was similar to that determined in previous experiments by Bezprozvanny and Ehrlich (1994). On the other hand, the mean open time of the $InsP_3R$ using Mn^{2+} as current carrier (4.1 ± 0.3 ms) was similar to that observed recently with Mg^{2+} as the permeating ion (4.3 ± 0.3 ms, Bezprozvanny and Ehrlich, 1994).

Regulation of the $InsP_3R$ by Cytosolic Mn^{2+}

To test the ability of cytosolic Mn^{2+} to substitute for Ca^{2+} in regulating the $InsP_3R$, we used exclusively 55 mM Ba^{2+} as the current carrier. After activation of the $InsP_3R$ with 0.5 mM ATP and 2 μM $InsP_3$, the concentration of Ca^{2+} or Mn^{2+} on the cytosolic side was increased stepwise (Fig. 4). The open probability of the $InsP_3R$ was very low at 10 nM free Ca^{2+} (pCa 8.0) or at 10 nM free Mn^{2+} (pMn 8.0). An increase in the cytosolic free Ca^{2+} concentration was followed by a rise in channel activation. The open probability peaked at 160 nM free Ca^{2+} (pCa 6.8, n = 5, Figs. 4 *A* and 5 *A*). Further additions of Ca^{2+} on the cytosolic side of the $InsP_3R$ led to a decrease in the open probability. The channel activity was virtually abolished by 1 μM free Ca^{2+} (pCa 6.0, n = 5, Figs. 4 *A* and 5 *A*). Thus, the open probability of the $InsP_3R$ depended upon cytosolic Ca^{2+} in a bell-shaped manner. This curve, generated with Ba^{2+} as the current carrier, is similar to the curve obtained with Ca^{2+} as the current carrier (Bezprozvanny et al., 1991).

Surprisingly, cytoplasmic Mn^{2+} was also able to regulate the open probability of the $InsP_3R$ in a bell-shaped manner. In contrast to the activation of this channel by cytosolic Ca^{2+}, the peak of the maximum channel activity was shifted to 630 nM free Mn^{2+} (pMn 6.2, n = 5; Figs. 4 *B*, 5 *B*). Channel activity was completely inhibited by 100 μM free Mn^{2+} (pMn 4.0; Figs. 4 *B*, 5 *B*). The activation and the inhibition of the $InsP_3$-gated channel by cytosolic Mn^{2+} indicate that this ion can bind to both modulatory Ca^{2+} binding sites of the $InsP_3R$.

To determine the affinities of Ca^{2+} and Mn^{2+} to the activation as well as to the inhibitory site of the $InsP_3R$, data were fitted by the equation (Bezprozvanny et al., 1991):

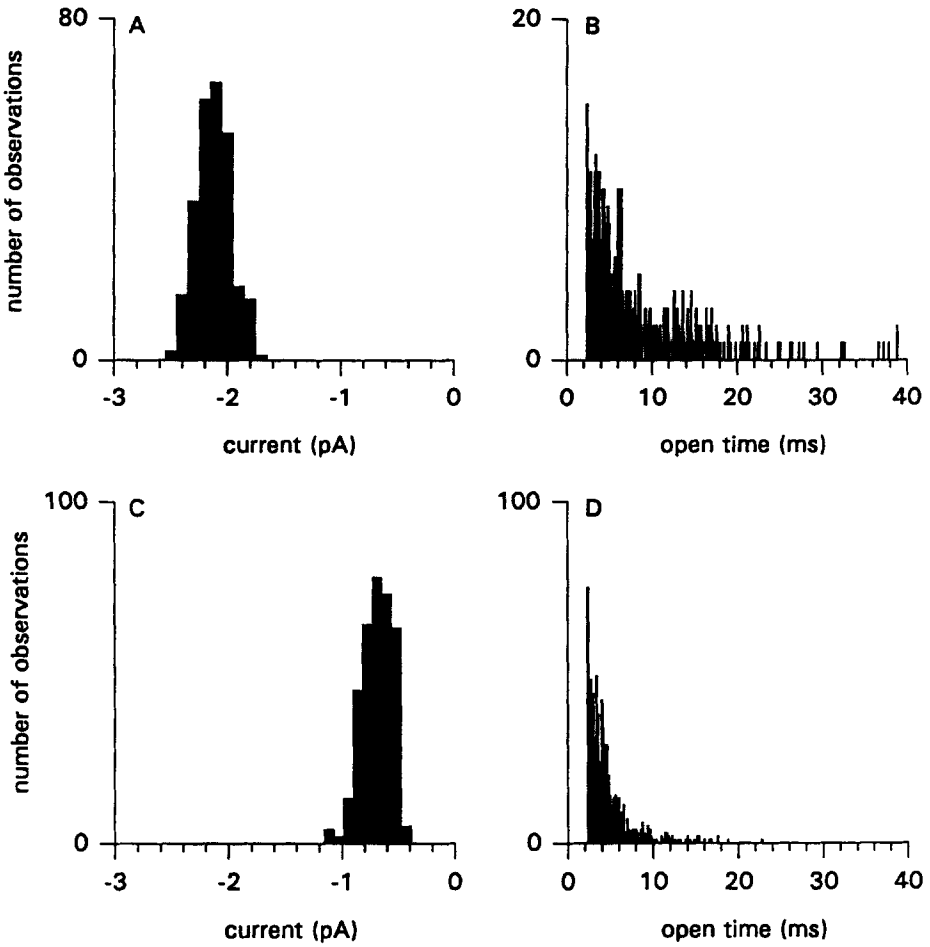

FIGURE 2. Comparison of $InsP_3$-gated channel openings with Ba^{2+} or Mn^{2+} as charge carriers. Current amplitude histograms (*A* and *C*) and open time distributions (*B* and *D*) were obtained from analysis of the experiments shown in Fig. 1. For *A* and *B*, Ba^{2+} was the current carrier. For *C* and *D*, Mn^{2+} was the current carrier.

$$P_0 = P_{max}\frac{[X^{2+}]^n k^n}{([X^{2+}]^n + K^n)([X^{2+}]^n + k^n)} \quad (1)$$

where P_{max} is the maximum open probability, K and k are the dissociation constants for the activating and inhibitory sites of the $InsP_3R$, respectively, and $[X^{2+}]$ is the free ion concentration (Ca^{2+} or Mn^{2+}) on the cytoplasmic side of the channel. The equation assumes that X^{2+} binds cooperatively to at least n binding sites at the $InsP_3R$. Although another model that does not assume cooperativity can describe the modulation of the $InsP_3R$ by Ca^{2+}, the fits to the data with the two models were indistinguishable (Bezprozvanny et al., 1991). Best fits were obtained with $n = 2.24$, $K = 143$ nM, $k = 155$ nM for Ca^{2+} and $n = 1.7$, $K = 176$ nM, $k = 2.3$ μM for Mn^{2+}. Thus, the affinity of the cytosolic activating site of the $InsP_3R$ for Ca^{2+} or Mn^{2+} is similar, whereas the affinity of the inhibitory site is ~15 times greater for Ca^{2+} than for Mn^{2+}. A consequence of the different affinities for the inhibitory site is that the width of the ion dependence curve is narrower for Ca^{2+} than for Mn^{2+}.

A comparison of the single channel characteristics of the maximally activated $InsP_3R$ (with Ba^{2+} as the current carrier) shows that the properties are similar regardless of the ion used to modulate the channel from the cytoplasmic side (Table II). When the channel was activated by 160 nM free Ca^{2+} (pCa 6.8) or 630 nM free Mn^{2+} (pMn 6.2) the mean current amplitude was indistinguishable (Table II). Furthermore, we calculated the maximum open probability for a single channel activated with each of these ions. At pCa 6.8 and pMn 6.2 the calculated maximum open probability was 0.029 and 0.024, respectively (Table II). Note that these values are the absolute open probability whereas the values shown in Fig. 5 are normalized to 1 (the highest open probability observed in each experiment).

TABLE I

Permeation of Ba^{2+} and Mn^{2+} through the IP_3R

Current carrier	Current	Mean open time	Conductance
	pA	*ms*	*pS*
55 mM Ba^{2+}	-2.2 ± 0.2 ($n = 4$)	8.9 ± 2.7 ($n = 4$)	88
55 mM Mn^{2+}	-0.8 ± 0.0 ($n = 3$)*	4.1 ± 0.3 ($n = 3$)‡	17

*$P < 0.001$, ‡$P < 0.01$ calculated using the heteroscedastic t test after revealing unequal variances by the f test

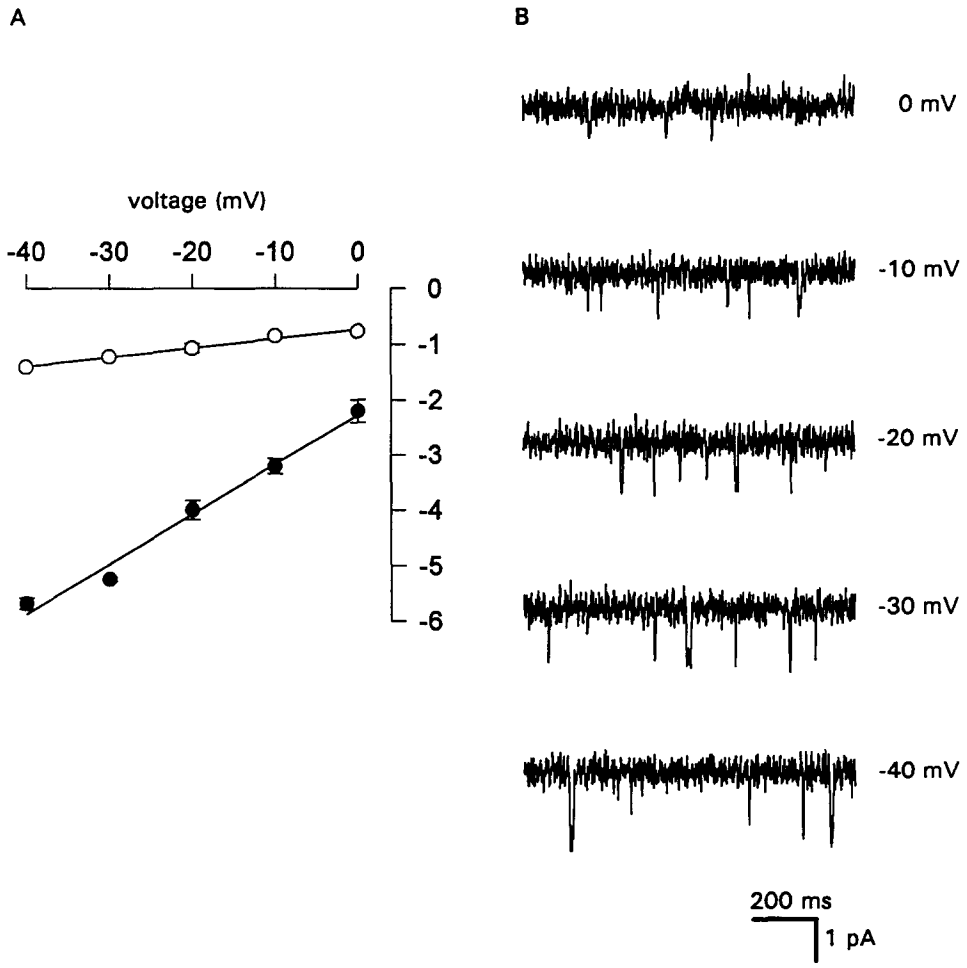

FIGURE 3. Single-channel current-voltage relationship with Ba^{2+} or Mn^{2+}. (*A*) Currents were monitored in the presence of 55 mM Ba^{2+} (●) or 55 mM Mn^{2+} (○) as the charge carrier on the luminal side of the channel. The $InsP_3R$ was activated as in Fig. 1. Individual points are the mean ± SEM ($n \geq 3$) of the current determined at transmembrane potentials between 0 mV and −40 mV. The single-channel conductance for each ion was determined as the slope of the current-voltage relationship and was 17 pS for Mn^{2+} and 88 pS for Ba^{2+}. (*B*) Current traces from one experiment done with 55 mM Mn^{2+} as charge carrier are shown.

DISCUSSION

We have investigated the ability of Mn^{2+} (*a*) to permeate through the $InsP_3R$ and (*b*) to substitute for cytosolic Ca^{2+} in modulating the activity of the channel. We found that Mn^{2+} can pass through the channel and that this ion can bind to both activating and inhibitory sites of the $InsP_3R$. In the following discussion, general conclusions will be made concerning the mechanism of ion permeation through the $InsP_3$-gated channel and the nature of the cytosolic binding sites for Ca^{2+} at the $InsP_3R$. Finally, the results will be discussed with respect to the common use of Mn^{2+} to quench the intracellular fluorescence of Ca^{2+} indicator dyes.

Ion Permeation through the $InsP_3R$

When Mn^{2+} was added to the luminal side of the $InsP_3R$, measurable channel currents were observed. As shown previously (Bezprozvanny and Ehrlich, 1994), currents through the $InsP_3R$ are not measurable under voltage clamp conditions if the concentration of the charge carrier is <1 mM. The contamination of the Mn^{2+} salt ($MnSO_4$) by other divalents was ≤0.005% (manufacturer information). Therefore, currents detected in the presence of 55 mM Mn^{2+} on the luminal side of the $InsP_3R$ must be the result of Mn^{2+} permeation through the $InsP_3R$.

The conductance of the $InsP_3$-gated channel for Mn^{2+} is smaller than for alkaline earth cations (Bezprozvanny and Ehrlich, 1994). Thus, Mn^{2+} can be added to the end of the permeation sequence of the $InsP_3R$: Ba^{2+} (2.2 pA, 88 pS) > Sr^{2+} (2.0 pA, 77 pS) > Ca^{2+} (1.4 pA, 53 pS) > Mg^{2+} (1.1 pA, 42 pS) > Mn^{2+} (0.8 pA, 17 pS). The order of permeation of the alkaline earth cations corresponds with the first of seven possible sequences predicted for divalent cation channels (Diamond and Wright, 1969). This sequence corresponds to the mobility of these ions in free solution and the standard free energy of hydration. Assuming that the $InsP_3R$ is a single ion channel (Bezprozvanny and Ehrlich, 1994), the narrowest region within the channel pore acts as the selectivity filter. Taking into consideration the permeation sequence of the alkaline earth cations through the $InsP_3R$, we can conclude that the channel pore, even at its narrowest point, has only a weak affinity with the permeating ion and, furthermore, that the free energy of hydration (which determines how easily the ion can slip off its water shell)

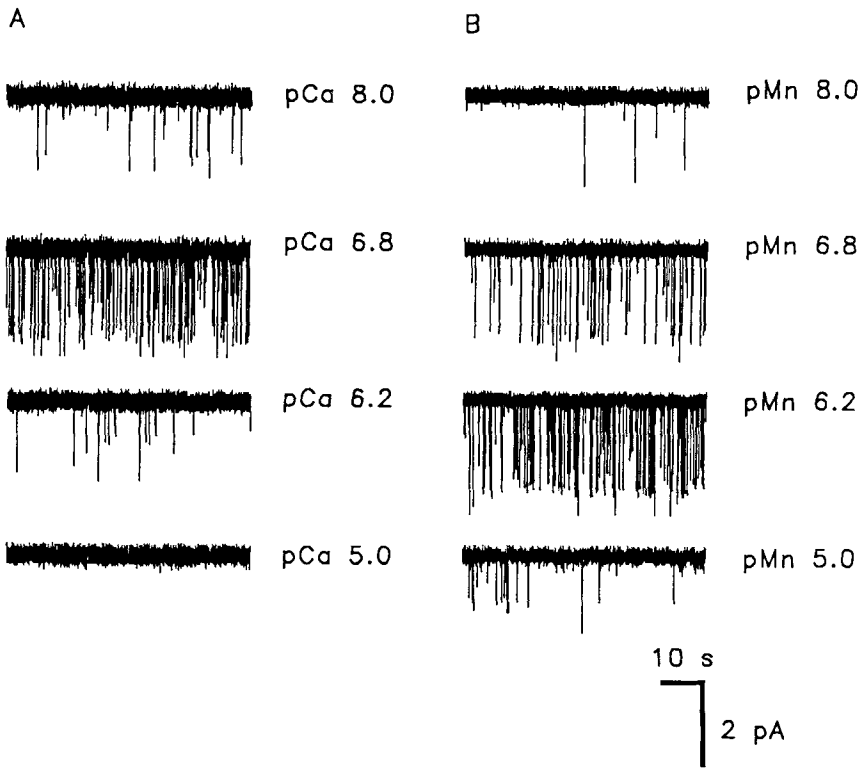

FIGURE 4. Single-channel currents through the $InsP_3R$ induced by cytosolic Ca^{2+} or cytosolic Mn^{2+}. Channel activity of the $InsP_3R$ in planar lipid bilayers was recorded in the presence of 0.5 mM ATP and 2 μM $InsP_3$. Ba^{2+} at 55 mM on the luminal side of the $InsP_3R$ was used as charge carrier. The free concentration of (*A*) Ca^{2+} or (*B*) Mn^{2+} on the cytosolic side of the channel was adjusted by addition of solutions of $CaCl_2$ and $MnSO_4$, respectively, to a solution containing 1 mM EGTA and 0.5 mM ATP. The free ion concentrations are given as the negative logarithm on the right side of each trace. Note that traces are shown on a compressed time scale when compared to Fig. 1. All traces were recorded at a transmembrane potential of 0 mV, and channel openings are indicated as downward deflections.

dominates the interaction between the ion and the pore surface.

From the Pauling radii and the free energies of hydration of Ba^{2+}, Sr^{2+}, Ca^{2+}, Mg^{2+}, and Mn^{2+} one would expect the conductance of the $InsP_3R$ for Mn^{2+} to be between the conductances for Ca^{2+} and Mg^{2+}. The radius of Mn^{2+} is 0.80 Å and the standard free energy of hydration is −1,828 kJ/mol at 25°C. These values for Mn^{2+} fall in the middle when compared to radii of 0.65 and 0.99 Å and free hydration energies of −1,902 and −1,589 kJ/mol for Mg^{2+} and Ca^{2+}, respectively (Edsall and McKenzie, 1978). However, Mn^{2+} passed through the channel more slowly than Mg^{2+}. The difference between theoretical and observed permeation sequence could be caused by the incompletely filled 3*d* orbital ($3d^5$) of Mn^{2+}. Consequently, oxygens (and nitrogens) from amino acid side chains and/or from the peptide backbone may provide coordinate binding sites for the permeating ion at the narrowest region of the channel pore. As a result of these interactions, the rate of Mn^{2+} passing through the channel would be slowed. On the other hand, the same oxygen-containing groups that build the "coordinate trap" for Mn^{2+} will interact more weakly with the alkaline earth cations and will aid in removing the hydration shell. Thus, permeation of the alkaline earth cations depends only on their free energy of hydration.

From this point of view it would be interesting to know the Mn^{2+} conductance of the ryanodine receptor, a second intracellular Ca^{2+} release channel. The ryanodine receptor shares many features with the $InsP_3R$, for example, a tetrameric organization (Anderson et al., 1989; Furuichi et al., 1989), ~40% identity of the transmembrane domain (Mignery et al., 1989), and similar conduction properties for divalent and monovalent cations (Tinker and Williams, 1992). An estimate of the permeability of the ryanodine receptor for Mn^{2+} would allow suggestions concerning the degree of similarity of the channel pore of these intracellular Ca^{2+} release channels.

In our experiments, Mn^{2+} was added to the luminal side of the $InsP_3$-gated channel. Thus, the measured Mn^{2+} current through the $InsP_3R$ corresponds to a Mn^{2+} flux directed from the lumen of the endoplasmic reticulum to the cytosol. Mn^{2+} current in the other direction (from the cytosol to the endoplasmic reticulum) was not measured. The magnitude of the current for all of the divalent cations at concentrations below 1 mM is too small to be detected with currently used bilayer techniques (Bezprozvanny and Ehrlich, 1994), and cytosolic Mn^{2+} concentrations above 1 mM inhibited the $InsP_3R$ (Fig. 4 *B* and Fig. 5 *B*). However, studies with the $InsP_3R$ and the ryanodine receptor have shown that these channels pass cation currents equally well in both directions (Mak and Foskett, 1994; Stehno-Bittel et al., 1995*a*; Tinker and Williams, 1992).

Effects of Cytosolic Mn^{2+} on the $InsP_3R$ Activity

There are two binding sites for Ca^{2+} on the $InsP_3R$ which are responsible for the regulation of the $InsP_3R$

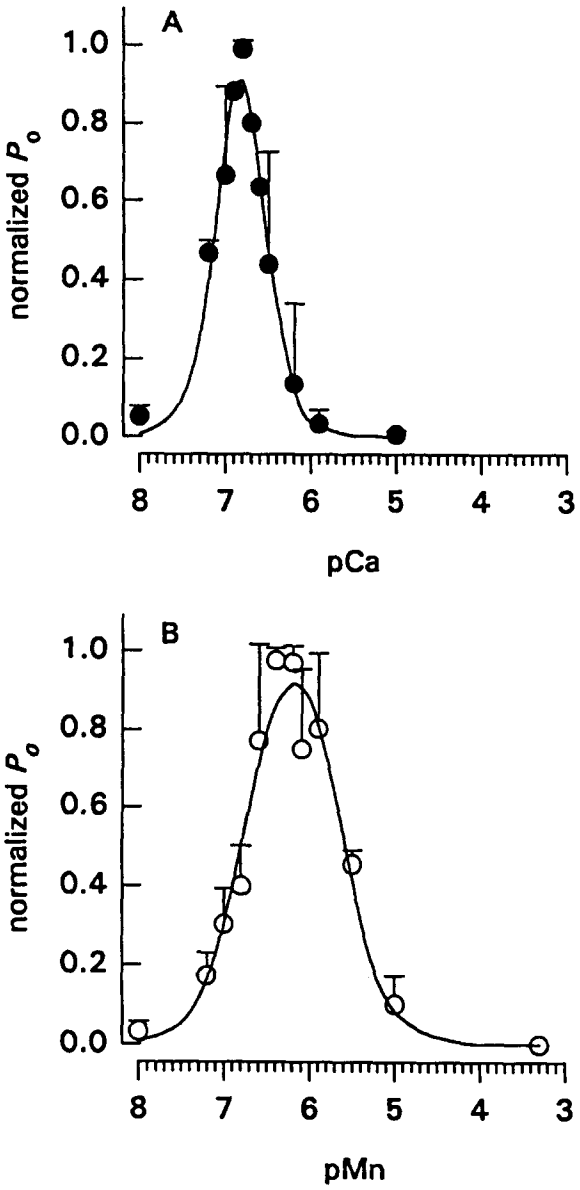

FIGURE 5. Bell-shaped dependence of $InsP_3R$-activity on the cytosolic concentration of Ca^{2+} or Mn^{2+}. Data were averaged from five experiments with increasing concentrations of (*A*) Ca^{2+} or (*B*) Mn^{2+} on the cytosolic side of the $InsP_3R$ (see Fig. 4). The open probability was normalized to the maximum open probability observed in each experiment. Recordings of at least 2 min for each free ion concentration were analyzed. Individual points are the mean ± SEM ($n \geq 3$), excluding the points at pCa 6.9, pCa 6.7, and pCa 6.6 in *A*, which represent only one experiment. Curves through the points were generated by curve fitting. See RESULTS for details about analysis and nonlinear regression. Best fits were obtained with $n = 2.24$, $K = 143$ nM, $k = 155$ nM and $n = 1.7$, $K = 176$ nM, $k = 2.3$ μM for Ca^{2+} and Mn^{2+}, respectively.

by cytosolic Ca^{2+}. We found that both sites are also affected by cytosolic Mn^{2+}. Unfortunately, the association constants of appropriate metal chelators (e.g. EGTA, HEDTA, NTA) are significantly larger for Mn^{2+} than for Ca^{2+}. Therefore, we were concerned that in the

TABLE II

Comparison of Single Channel Currents through the $InsP_3R$ Induced by Cytosolic Ca^{2+} or Cytosolic Mn^{2+}

Cytosolic ion	Current carrier	Current	Open time	Open probability*	*n*
		pA	*ms*		
160 nM Ca^{2+}	55 mM Ba^{2+}	−2.2 ± 0.2	8.9 ± 2.7	0.029 ± 0.016	4
630 nM Mn^{2+}	55 mM Ba^{2+}	−2.0 ± 0.1	8.2 ± 2.3	0.024 ± 0.008	4

*Note that the absolute open probability is given in this table, whereas the values used in Fig. 5 are normalized to 1 (the maximum open probability observed in each experiment).

case of stepwise additions of Mn^{2+} (Fig. 4 *A* and Fig. 5 *B*), contamination of Ca^{2+}, released from the chelator after addition of Mn^{2+}, may be responsible for the observed activation and inhibition of the $InsP_3R$ in these experiments. To directly test this possibility, the Ca^{2+} contamination in all the solutions used was determined by atomic absorption spectroscopy. Total Ca^{2+} concentrations between 0.5 and 1 μM in our "Ca^{2+} free" solutions were obtained. With these results we calculated the free Ca^{2+} concentration on the cytosolic side of the $InsP_3R$ after each stepwise addition of Mn^{2+} using a computer algorithm (Fabiato, 1988) and assuming a Ca^{2+} contamination of 1 μM total calcium in the solutions. At pMn 6.2, where the $InsP_3R$ was maximally activated, a free Ca^{2+} concentration of pCa 8.0 was obtained. As shown in Fig. 5 *A*, this pCa is too low to stimulate the $InsP_3R$. Thus, the observed activation of the $InsP_3$-gated channel at pMn 6.2 must be caused by Mn^{2+}. Furthermore, at pMn 5.0 when the $InsP_3R$ was inhibited, a pCa of 6.9 was calculated. In this case, pCa 6.9 is too low to be responsible for the observed inhibition of the $InsP_3R$ at pMn 5.0. Rather, a pCa of 6.9 should allow optimal channel activation (Fig. 5 *A*). The finding that at pMn 5.0 (which corresponds to pCa 6.9) channel inhibition was observed, leads to two conclusions: (*a*) Mn^{2+} must be responsible for the channel inhibition, and (*b*) Ca^{2+} can not activate the $InsP_3R$ if the inhibitory site is already occupied by Mn^{2+}.

Taken together, we suggest that Mn^{2+} is able to bind to both regulatory Ca^{2+} binding sites of the $InsP_3R$. As a result of these interactions, the open probability of the $InsP_3$-gated channel is affected by cytosolic Mn^{2+} in a bell-shaped manner. The dissociation constant of the activating site of the $InsP_3R$ for Mn^{2+} is similar to Ca^{2+} (K_{Mn} = 176 nM and K_{Ca} = 143 nM). On the other hand, the affinity of the inhibitory site is ~15 times lower for Mn^{2+} than for Ca^{2+} (k_{Mn} = 2.3 μM, k_{Ca} = 155 nM). Thus, the ability of Mn^{2+} to replace Ca^{2+} in regulating the channel activity differs for the two regulatory binding sites of the $InsP_3R$.

In this context it is interesting that Sr^{2+} influences the $InsP_3$-gated Ca^{2+} release in liver and sheep cerebel-

lum in a manner similar to that reported in this study for Mn^{2+} (Hannaert-Merah et al., 1995; Marshall and Taylor, 1994). Marshall and Taylor (1994) reported EC_{50}'s of 570 nM Sr^{2+} and ~900 μM Sr^{2+} for the sensitization and inhibition of $^{45}Ca^{2+}$ release through the $InsP_3R$ from liver microsomes. Similar results have been shown recently for the cerebellar $InsP_3R$ by Hannaert-Merah et al. (1995). In contrast to Ca^{2+}, Mn^{2+}, or Sr^{2+}, cytosolic Ba^{2+} is only a very poor activator of the $InsP_3R$ and does not have inhibitory effects on the channel activity (Hannaert-Merah et al., 1995; Marshall and Taylor, 1994). Considering these findings and our results in the present study, the affinity sequences for the two regulatory binding sites on the cytosolic site of the $InsP_3R$ are: activation site, $Ca^{2+} \equiv Mn^{2+} > Sr^{2+} >> Ba^{2+}$; inhibitory site, $Ca^{2+} > Mn^{2+} >> Sr^{2+} >> Ba^{2+}$. Because the two Ca^{2+} binding sites of the $InsP_3R$ have different affinities for the divalent cations, we conclude that activation and inhibitory sites must be structurally different.

The selectivity sequence for the inhibitory site can be used to explain the duration of the mean open time of the channel for the various divalent cations. When the mean open time was estimated using the same cytosolic conditions to activate the $InsP_3R$ but different ions were present on the luminal side to carry the current (this study and Bezprozvanny and Ehrlich, 1994), the sequence was: Ca^{2+} (2.9 ± 0.2 ms) < Mn^{2+} (4.1 ± 0.3 ms) < Sr^{2+} (5.9 ± 1.6 ms) < Ba^{2+} (8.9 ± 2.9 ms). This order does not correspond to the relative current magnitude but is instead related to the affinity for the inhibitory site. The ability of Ca^{2+} in the vicinity of an open channel pore to inhibit channel activity has been predicted in several models (Bezprozvanny and Ehrlich, 1994; Jong et al., 1993; Stern, 1992). Our results support these predictions. The higher the affinity of the permeating ion on the modulatory site on the $InsP_3R$, the sooner the "outcoming" ion can bind to the inhibitory site and the shorter the open time of the channel will be.

Conclusions with Respect to the Use of Mn^{2+} as a Tool for Studying Intracellular Calcium Signaling

Mn^{2+} binds to the fluorescent Ca^{2+} indicator dyes (e.g., fura-2, indo-1) with high affinity, followed by an immediate and strong quenching of the dye fluorescence (Grynkiewicz et al., 1985). This property has made

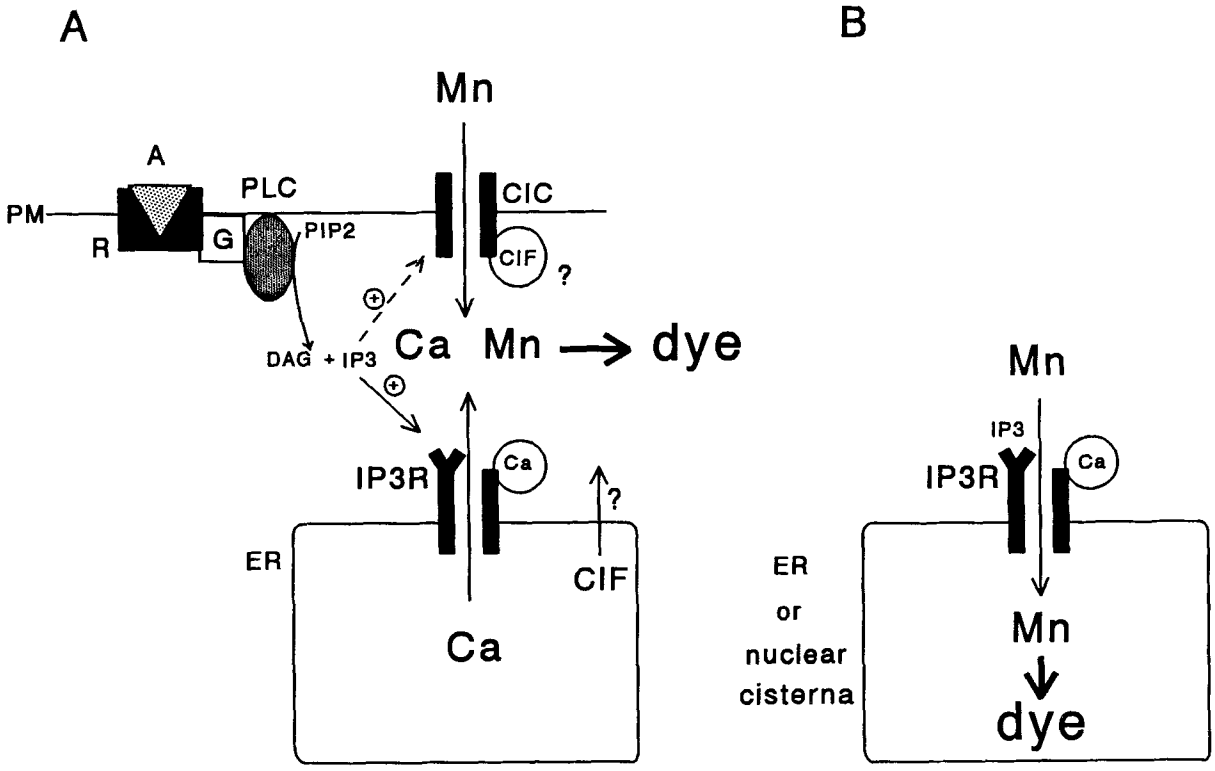

FIGURE 6. Mn^{2+} as a tool for studying intracellular calcium signaling. Mn^{2+} has been used to quench the fluorescence of Ca^{2+} indicator dyes in different experiments: (*A*) to discriminate between the Ca^{2+} entry through a ligand-gated channel in the plasma membrane and the release of stored Ca^{2+} from the endoplasmic reticulum and (*B*) to study or to detect the $InsP_3R$ in dye-loaded organelles. Abbreviations used are: *CIC*, ligand-gated Ca^{2+} influx channel; *PM*, plasma membrane; *ER*, endoplasmic reticulum; *R*, receptor; *A*, agonist; *G*, G-protein; *PLC*, phospholipase C; *PIP2*, phosphatidyl inositol 4,5-bisphosphate; *DAG*, diacylglycerol; *IP_3*, inositol 1,4,5-trisphosphate; *IP_3R*, IP_3-receptor; *CIF*, Ca^{2+} influx factor.

Mn^{2+} a useful tool to discriminate between the activation of a Ca^{2+} influx channel in the plasma membrane (that is also permeable for Mn^{2+}) and the release of stored Ca^{2+} by the $InsP_3R$. The activation of the Ca^{2+} entry pathway can be observed by the Mn^{2+}-induced quenching of cytosolic dye fluorescence (Fig. 6 *A*, Merritt et al., 1989).

This study allows two conclusions concerning these experiments. First, because of its ability to pass through the $InsP_3R$, Mn^{2+} could also enter the endoplasmic reticulum (see Fig. 6 *A*). If cells are loaded with a membrane-permeable dye, dye accumulation within intracellular compartments can occur easily (Glennon et al., 1992; Kass et al., 1994). This accumulation may be critical for studies of the Ca^{2+} influx channel in the plasma membrane. If the rate of Mn^{2+} flux through the $InsP_3R$ is the rate-limiting step compared to the entry of Mn^{2+} into the cytosol, the fluorescence quenching would depend exclusively on the $InsP_3R$. Under these conditions, the measured rate of fluorescence quenching does not reflect the activation of the Ca^{2+} influx pathway.

The second conclusion has implications for the function of the $InsP_3R$ in quenching experiments. After cellular stimulation, the influx of extracellular Mn^{2+} into the cytosol should not alter the activation and inhibition of the $InsP_3R$. This lack of effect on $InsP_3R$ function is a consequence of the similar affinity of the activating Ca^{2+} binding site for Ca^{2+} and Mn^{2+}. Consequently, these ions are equipotent as coactivators of the $InsP_3R$. Thus, the activation of the $InsP_3R$ should not be affected by the presence of Mn^{2+} in the extracellular medium. On the other hand, the regulatory Ca^{2+} binding site of the $InsP_3R$ responsible for channel inactivation has a significantly higher affinity for Ca^{2+} over Mn^{2+}. Therefore, Ca^{2+} released from its intracellular store will inhibit the $InsP_3R$ before the cytosolic Mn^{2+} concentration is high enough to bind to the inhibitory binding site of the channel. The conclusion that the regulation of the $InsP_3R$ is not altered by Mn^{2+} is of special importance if the $InsP_3R$ itself is involved in the regulation of the Ca^{2+} influx pathway by a store-dependent capacitative mechanism (Putney, 1990).

In addition to studies of the Ca^{2+} influx pathway, Mn^{2+} has also been used to investigate the $InsP_3R$ in permeabilized cells or in isolated nuclei by quenching intraorganellar (endoplasmic reticulum, nuclear cisterna) dye fluorescence (Fig. 6 *B*; Hajnoczky and Thomas, 1994; Stehno-Bittel et al., 1995b). In these studies it was assumed that Mn^{2+} is able to permeate through the $InsP_3R$ when the channel is activated by $InsP_3$. However, the Mn^{2+} permeability of the $InsP_3R$ had not been demonstrated. More importantly, our finding that high concentrations of Mn^{2+} ($\geq$10 μM) inhibit the $InsP_3R$ may have consequences for this type of experiment. Hajnoczky and Thomas (1994) used 2 μM free Mn^{2+} to monitor the function of the $InsP_3R$. From the data obtained in the present study, this Mn^{2+} concentration, although already on the inhibitory phase of the curve, is appropriate to investigate the $InsP_3$-gated channel. On the other hand, in a recent paper by Stehno-Bittel et al. (1995*b*) experiments were described that used 10 μM $MnCl_2$ to quench the mag-indo-1 fluorescence within the nuclear cisterna from *Xenopus leavis* oocytes. The apparent contradiction between this work and our results may have two explanations. First, the Mn^{2+} concentration given by Stehno-Bittel et al. (1995*b*) reflects total values. The concentration of free Mn^{2+} could be lower than 10 μM due to buffering compounds in the media used. Second, differences in the primary sequence of the $InsP_3R$ from cerebellum and oocytes may be responsible for the different effects of Mn^{2+} on the channel activity. For instance, the maximum activation of the $InsP_3R$ from oocytes is slightly shifted to higher Ca^{2+} concentrations (pCa 6.0, Stehno-Bittel et al., 1995b) compared to the cerebellar $InsP_3R$ (pCa 6.8, this paper and Bezprozvanny et al., 1991). This shift suggests there may be a similar shift in the affinities of the two regulatory Ca^{2+} binding sites to Mn^{2+} in oocytes.

In summary, we found that Mn^{2+} can pass through the $InsP_3R$ and that it is a potent modulator of this channel. Despite these properties, Mn^{2+} remains a useful tool for investigating Ca^{2+} homeostasis, as long as appropriate concentrations are used.

We thank E. Kaftan and K. Quinn for helpful discussions as these experiments progressed. Comments on the manuscript by W.K. Chandler, L.B. Cohen, J. Watras, and I. Bezprozvanny are gratefully acknowledged. Our special thanks go to W. Dyckman, C.-Z. Chen, and P. Ardery at Hartford Hospital for their very friendly assistance in obtaining canine cerebella.

This work was supported by a Grant-in-Aid from the Patrick and Catherine Weldon Donaghue Medical Research Foundation, National Institutes of Health grant GM 51480, and a DAAD fellowship to F. Striggow.

Original version received 1 March 1996 and accepted version received 1 May 1996.

REFERENCES

Anderson, K., F.A. Lai, Q.-Y. Liu, E. Rousseau, H.P. Erickson, and G. Meissner. 1989. Structural and functional characterization of the purified cardiac ryanodine receptor-Ca^{2+} release channel complex. *J. Biol. Chem.* 264:1329–1335.

Berridge, M.J. 1993. Inositol trisphosphate and calcium signaling. *Nature (Lond.).* 361:315–325.

Bezprozvanny, I., and B.E. Ehrlich. 1994. Inositol (1,4,5)-trisphosphate gated Ca channels from canine cerebellum: divalent cation conduction properties and regulation by intraluminal Ca. *J. Gen. Physiol.* 104:821–856.

Bezprozvanny, I., and B.E. Ehrlich. 1993. ATP modulates the function of inositol 1,4,5-trisphosphate-gated channels at two sites. *Neuron.* 10:1175–1184.

Bezprozvanny, I., J. Watras, and B.E. Ehrlich. 1991. Bell-shaped calcium-response curves of $Ins(1,4,5)P_3$- and calcium-gated channels from endoplasmic reticulum of cerebellum. *Nature (Lond.).* 351:751–754.

Charles, A.C. 1994. Glia-neuron intercellular calcium signaling. *Dev. Neurosci.* 16:196–206.

Clapham, D. 1995. Calcium signalling. *Cell.* 80:259–268.

Diamond, J.M., and E.M. Wright. 1969. Biological membranes: the physical basis of ion and nonelectrolyte selectivity. *Annu. Rev. Physiol.* 31:581–646.

Edsall, J.T., and H.A. McKenzie. 1978. Water and proteins. I. The significance of water; its interaction with electrolytes and nonelectrolytes. *Adv. Biophys.* 10:137–207.

Fabiato, A. 1988. Computer programs for calculating total from specified free or free from specified total ionic concentrations in aqueous solutions containing multiple metals and ligands. *Methods Enzymol.* 157:378–417.

Finch, E.A., T.J. Turner, and S.M. Goldin. 1991. Calcium as a coagonist of inositol 1,4,5-trisphosphate-induced calcium release. *Science (Wash. DC).* 252:443–446.

Furuichi, T., S. Yoshikawa, A. Miyawaki, K. Wada, N. Maeda, and K. Mikoshiba. 1989. Primary structure and functional expression of the inositol 1,4,5-trisphosphate-binding protein P400. *Nature (Lond.).* 342:32–38.

Ghosh, T.K., P.S. Eis, J.M. Mullaney, C.L. Ebert, and D.L. Gill. 1988. Competitive, reversible, and potent antagonism of inositol 1,4,5-trisphosphate-activated calcium release by heparin. *J. Biol. Chem.* 263:11075–11079.

Glennon, M.C., G.S.J. Bird, C.-Y. Kwan, and J.W. Putney. 1992. Actions of vasopressin and the Ca^{2+}-ATPase inhibitor, thapsigargin, on Ca^{2+} signaling in hepatocytes. *J. Biol. Chem.* 267:8230–8233.

Grynkiewicz, G., M. Poenie, and R.Y. Tsien. 1985. A new generation of Ca indicators with greatly improved fluorescence properties. *J. Biol. Chem.* 260:3440–3450.

Hajnoczky, G., and A.P. Thomas. 1994. The inositol trisphosphate calcium channel is inactivated by inositol trisphosphate. *Nature (Lond.).* 370:474–477.

Hannaert-Merah, Z., L. Combettes, J.-F. Coquil, S. Swillens, J.-P. Mauger, M. Claret, and P. Champeil. 1995. Characterization of the co-agonist effects of strontium and calcium on myo-inositol trisphosphate-dependent ion fluxes in cerebellar microsomes. *Cell Calcium.* 18:390–399.

Horn, R. 1991. Estimating the number of channels in patch recordings. *Biophys. J.* 60:433–439.

Iino, M. 1990. Biphasic Ca^{2+} dependence of inositol 1,4,5-trisphosphate–induced Ca release in smooth muscle cells of the guinea pig *taenia caeci. J. Gen. Physiol.* 95:1103–1122.

Jong, D.-S., P.C. Pape, W.K. Chandler, and S.M. Baylor. 1993. Reduction of calcium inactivation of sarcoplasmic reticulum calcium release by Fura-2 in voltage-clamped cut twitch fibers from frog muscle. *J. Gen. Physiol.* 102:333–370.

Kass, G.E.N., D.-C. Webb, S.C. Chow, J. Llopis, and P. O. Berggren. 1994. Receptor-mediated Mn^{2+} influx in rat hepatocytes: comparison of cells loaded with fura-2 ester and cells microinjected with fura-2 salt. *Biochem. J.* 302:5–9.

Mak, D.-O., and J.K. Foskett. 1994. Single-channel inositol 1,4,5-trisphosphate receptor currents revealed by patch clamp of isolated *Xenopus* oocyte nuclei. *J. Biol. Chem.* 269:29375–29378.

Malenka, R.C. 1994. Synaptic plasticity in the hippocampus: LTP and LTD. *Cell.* 78:535–538.

Marshall, I., and C. Taylor. 1994. Two calcium binding sites mediate the interconversion of liver inositol 1,4,5-trisphosphate receptors between three conformations states. *Biochem. J.* 301:591–598.

Merritt, J.E., R. Jacob, and T.J. Hallam. 1989. Use of manganese to discriminate between calcium influx and mobilization from internal stores in stimulated human neutrophils. *J. Biol. Chem.* 264: 1522–1527.

Mignery, G., T.C. Sudhof, K. Takei, and P. De Camilli. 1989. Putative receptor for inositol 1,4,5-trisphosphate similar to ryanodine receptor. *Nature (Lond.).* 342:192–195.

Putney, J.W., Jr. 1990. Capacitative calcium entry revisited. *Cell Calcium.* 11:611–624.

Sneyd, J., B.T. Wetton, A.C. Charles, and M.J. Sanderson. 1995. Intercellular calcium waves mediated by diffusion of inositol trisphosphate: a two-dimensional model. *Am. J. Physiol.* 268:C1537–C1545.

Stehno-Bittel, L., A. Luckhoff, and D.E. Clapham. 1995*a*. Calcium release from the nucleus by $InsP_3$ receptor channels. *Neuron.* 14: 163–167.

Stehno-Bittel, L., C. Perez-Terzic, and D. Clapham. 1995*b*. Diffusion across the nuclear envelope inhibited by depletion of the nuclear Ca^{2+} store. *Science (Wash. DC).* 270:1835–1838.

Stern, M.D. 1992. Buffering of calcium in the vicinity of a channel pore. *Cell Calcium.* 13:183–192.

Supattapone, S., P.F. Worley, J.M. Baraban, and S.H. Snyder. 1988. Solubilization, purification, and characterization of an inositol trisphosphate receptor. *J. Biol. Chem.* 263:1530–1534.

Tinker, A., and A.J. Williams. 1992. Divalent cation conduction in the ryanodine receptor of sheep cardiac muscle sarcoplasmic reticulum. *J. Gen. Physiol.* 100:479–493.

Watras, J., I. Bezprozvanny, and B.E. Ehrlich. 1991. Inositol 1,4,5-trisphosphate-gated channels in cerebellum—presence of multiple conductance states. *J. Neurosci.* 11:3239–3245.